Korean J. Chem. Eng., 36(11), 1854-1858 (2019)
DOI: 10.1007/s11814-019-0362-3

pISSN: 0256-1115
eISSN: 1975-7220

RAPID COMMUNICATION

Enhancing membrane wetting resistance through superhydrophobic modification by polydimethylsilane-grafted-SiO_2 nanoparticles

Moau Jian Toh*, Pei Ching Oh*,†, Abdul Latif Ahmad, and Julien Caille*****

*CO_2 Research Centre, Institute of Contaminant Management, Chemical Engineering Department, Universiti Teknologi PETRONAS, 32610 Seri Iskandar, Perak, Malaysia
**School of Chemical Engineering, Engineering Campus, Universiti Sains Malaysia, 14300 Nibong Tebal, Penang, Malaysia
***National Superior Engineering School of Industrial Technologies, 64000 Pau, France
(*Received 5 April 2019 • accepted 15 August 2019*)

Abstract−Membrane gas-liquid separation technology has been widely employed in membrane filtration, distillation, and gas absorption, attributed to its high mass transfer efficiency. However, hydrophobic membranes may suffer from pore wetting at low operational pressure difference, leading to the deterioration of removal flux. Hence, anti-wetting strategy via membrane surface modification to improve its intrinsic hydrophobicity needs to be investigated. In this work, modified superhydrophobic polyvinylidene fluoride-co-hexafluoropropylene (PVDF-HFP) membrane was synthesized via non-solvent induced phase separation. Polydimethylsilane-grafted-silica (PGS) nanoparticles with non-polar Si-O-Si bonds were used as surface modifier in coagulation bath to enhance membrane surface hydrophobicity. Results demonstrated that the addition of nanoparticles improved the surface roughness via formation of hierarchical structure. Additionally, the deposition of nanoparticles on polymer spherulites significantly reduced the surface free energy. As a result, modified membranes achieved superhydrophobicity with water contact angle exceeding 150°. The stability tests also showed that the deposition layer of modified membrane was mechanically and thermally robust. This superhydrophobic modification by PGS nanoparticles is an advanced and facile approach to alleviate membrane wetting.

Keywords: Superhydrophobic Surface, Wetting Resistance, Hierarchical Morphology, Grafted-silica Nanoparticles

INTRODUCTION

In membrane gas-liquid separation, hydrophobic membranes act as a physical barrier between gas and liquid by allowing the diffusion of gas molecules through the non-wetted pores. Nevertheless, its non-wetted condition may transform to partially wetted or wetted mode when the pressure difference in the system exceeds the liquid entry pressure of the membrane [1]. Such condition imposes significant mass transfer resistance on the overall removal process, leading to the deterioration of gas removal flux in liquid-occupied pores. To secure effective gas removal process, the pores of the membrane need to be gas-filled [2]. This has called for the enhancement of membrane hydrophobicity towards superhydrophobic surface to mitigate the tendency of membrane wetting. Attributed to its superior anti-wettability, superhydrophobic membrane enhances the removal flux and operational stability compared to hydrophobic membrane [3].

One of the effective approaches to render superhydrophobicity involves surface modification to lower surface free energy and induce hierarchical structure in the membrane [4,5]. This can be achieved by incorporating silane-modified inorganic nanoparticles as non-solvent additive in a coagulation bath [6]. Modified nanoparticles are intrinsically hydrophilic, wherein the water-reactive hydroxyl groups are deactivated via surface grafting with the silane. During phase inversion process, nanoparticles induce the formation of hierarchical spherulitic particles and alter the surface chemistry, hence endowing the membrane with superhydrophobicity.

To the best of our knowledge, no research has been done on superhydrophobic modification induced by non-solvent additive of polydimethylsilane-grafted-silica (PGS) nanoparticles. In this study, we reported superhydrophobic modification using PGS nanoparticles in coagulation bath via non-solvent induced phase separation. The effect of PGS nanoparticles on modified membranes' morphology, surface roughness, surface energy, and contact angle were studied. The stability of the modified membranes was also investigated.

EXPERIMENTAL

1. Materials and Membrane Preparation

Polyvinylidene fluoride-co-hexafluoropropylene (PVDF-HFP) pellets were purchased from Sigma Aldrich, USA. Polydimethylsilane-grafted-silica (PGS) nanoparticles were supplied courtesy of Wacker, Germany. The superhydrophobic membrane was developed by non-solvent induced phase separation. PVDF-HFP polymer pellets were dried at 60 °C in vacuum oven for 24 h to remove moisture [7]. The dope solution was prepared by dissolving PVDF-HFP pellets in NMP solvent at 70 °C for 24 h. The resulting dope solution was sonicated for 4 h to remove trapped air bubbles and kept overnight [8]. Coagulation bath using 0, 1, 2, 3, 4, 5 and 6 gL^{-1} of PGS nanoparticles in ethanol was prepared by stirring at room

†To whom correspondence should be addressed.
E-mail: peiching.oh@utp.edu.my

temperature for 24 h. The corresponding membrane samples were denoted as M-0, M-1, M-2, M-3, M-4, M-5 and M-6, respectively. The dope solution was cast on a glass plate and immersed in coagulation bath for 24 h. Then the membrane was removed from the glass plate and air-dried.

2. Membrane Characterization

The surface and cross section morphology of membranes was characterized by scanning electron microscopy (Tabletop Microscope TM3030 Hitachi, Japan). The cross section was obtained by fracturing the membrane samples in liquid nitrogen. Energy dispersive X-ray spectroscopy (EDX) was performed for Si surface elemental analysis. Contact angle measurement on the membrane surface was conducted using a goniometer (Rame-hart 260, USA) via the sessile drop technique. Distilled water (10 μL) was dropped through the needle of a micro-syringe to the membrane surface. The droplet images were analyzed by a processing software to obtain the contact angle via Laplace-Young equation. The average value was reported from five measurements. The surface free energy of the membrane was determined by geometric mean method [9]. In this approach, the contact angle of water and diiodomethane on membrane surface were measured. The surface free energy was calculated from a set of two first-order linear equations. The average surface roughness, R_a of the membrane surface was analyzed using 3D SEM imaging. The measurements were performed at scan area of 50 μm×50 μm. The average value was obtained from three measurements.

3. Thermal and Mechanical Stability

To investigate the stability of modified membranes, mechanical and thermal tests were conducted. The mechanical stability of the membranes was analyzed by immersing the sample in distilled water and sonicated for 2 h at ambient condition. For thermal stability, membranes were immersed in distilled water at 90 °C for 2 h [10]. All samples were air-dried prior to water contact angle measurement. The durability tests were performed for four cycles and the average value from at least two measurements was reported.

RESULTS AND DISCUSSION

Fig. 1 and 2 depict the scanning electron micrographs of synthesized membranes' surface and cross-section. Unmodified membrane, M-0, which was prepared without PGS nanoparticles, induced a microporous structure composed of polymer spherical glob-

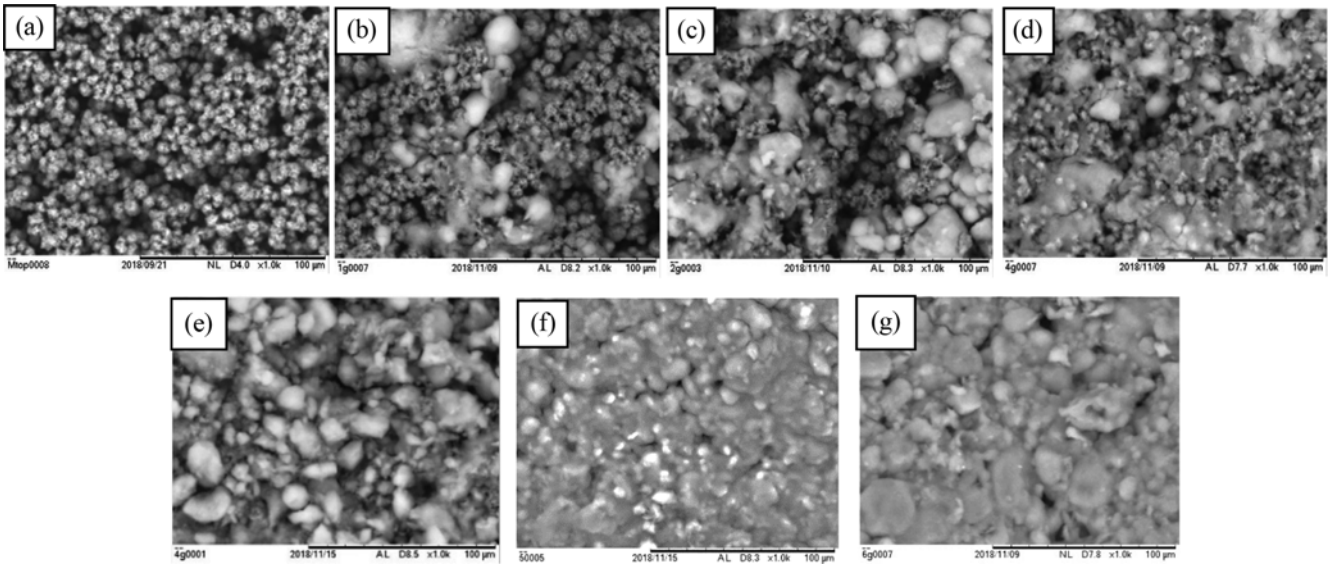

Fig. 1. Surface morphology of (a) M-0, (b) M-1, (c) M-2, (d) M-3, (e) M-4, (f) M-5, and (g) M-6 membrane at 1K magnification.

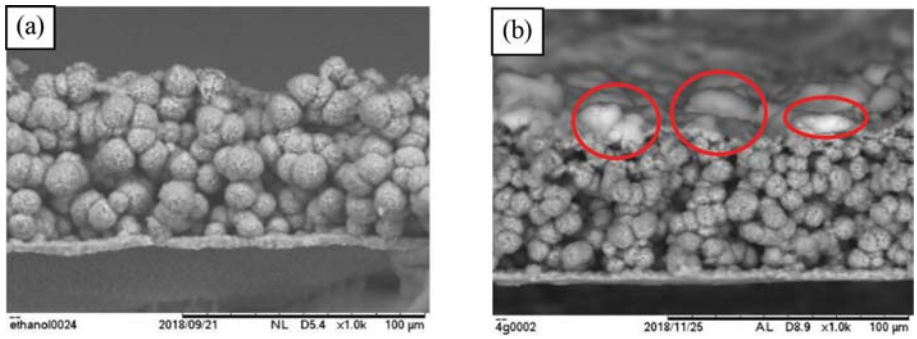

Fig. 2. Cross section morphology of (a) M-0, and (b) M-4 membrane at 1K magnification. Red circles denote the attachment of PGS nanoparticles on membrane surface.

ules. Such structure was derived from the solid-liquid demixing (crystallization) process, wherein the crystallizable segments of the polymer induced the growth of nodular crystalline particles [11]. After which all crystalline particles nucleated to a similar size and merged to form bi-continuous structure in the membrane. Similar morphology was reported by Munirasu et al. [12]. This was due to the poor coagulation ability of ethanol which delayed the precipitation rate and allowed a great extent of polymer crystallization to occur during immersion process. Therefore, crystallization-dominated morphology was observed in ethanol induced membranes.

Surface modification by incorporating PGS nanoparticles resulted in the attachment of non-uniform clusters on the membrane microporous surface. As depicted in cross-section morphology (Fig. 2(b)), the PGS nanoparticles were densely distributed on the skin layer of modified membrane. The deposition of these nanoparticles was not smooth but formed multilevel protrusions on the surface. As the PGS loading increased, the surface of the modified membrane was gradually covered with a layer of PGS nanoparticles. In a separate study by Wu et al. for PVDF membranes, densely attached nanoparticles were observed when modified silica was incorporated in coagulation bath [6]. This could be explained by the migration of PGS nanoparticles onto the polymer film accompanying solvent-nonsolvent exchange. Subsequently, the nanoparticles agglomerated into non-uniform clusters and deposited on membrane surface, forming a hierarchical structure with multilevel roughness.

Table 1. Si elemental composition and porosity of membrane

Membrane	Si composition (%)
M-0	-
M-1	12.66
M-2	17.35
M-3	23.46
M-4	41.67
M-5	44.7
M-6	44.53

The surface elemental analysis of the PVDF-HFP membrane is shown in Table 1. The Si composition increased from 12.66% to 44.7% in membrane samples M-1 to M-5. This is consistent with SEM morphology that showed enhanced PGS attachment on the polymer nodular particles. Further increase in PGS beyond 5 gL^{-1}, shows only slight increase in Si composition as the surface was saturated with a hierarchical layer of agglomerated cluster.

The three-dimensional images and average surface roughness, R_a of the membranes are demonstrated in Fig. 3. The lowest R_a of 1.68±0.22 μm was found in the unmodified membrane due to the uniform distribution of polymer globules in the structure. The intro-

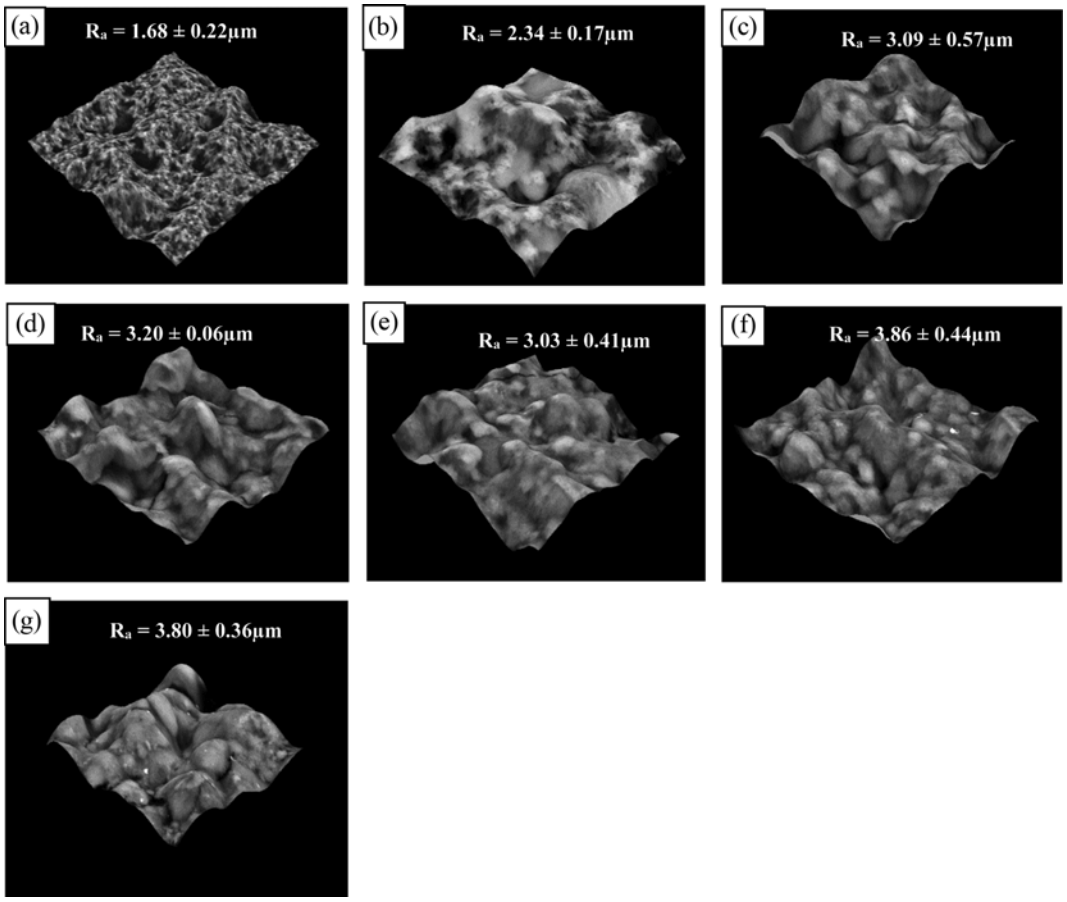

Fig. 3. Surface topography and average surface roughness of (a) M-0, (b) M-1, (c) M-2, (d) M-3, (e) M-4, (f) M-5, and (g) M-6 membrane at 1K magnification.

duction of PGS nanoparticles resulted in the deposition of nanoparticles on polymer particles, which led to the increased protrusion and valley regions on the membrane surface. As shown in Fig. 3(b) to (g), lumpy aggregates were visible in the 3D images of all modified membranes. The average surface roughness of all modified membranes was significantly enhanced. The highest average surface roughness was achieved by the modified membrane, M-5 at 3.86±0.44 μm, showing 56.6% improvement compared to unmodified membrane. As can be seen, the surface roughness was not significantly affected by the PGS loading, which may be due to the inhomogeneous distribution of nanoparticles on modified membrane surface.

The surface free energy of membranes determined using geometric mean approach are shown in Fig. 4. Unmodified membrane, M-0, shows the highest surface free energy of 8.17±0.29 mNm^{-1}, indicating the highest surface polarity and dispersive force on membrane surface [13]. Hence, the unmodified membrane with high surface free energy is highly prone to interacting with liquid component and causes pore wetting. With the increase in PGS nanoparticles deposited on polymer spherulites from M-1 to M-5, the surface free energy decreased from 2.58±0.06 mNm^{-1} to 0.68±0.09 mNm^{-1}. This is due to the steric hindrance introduced by non-polar bonds Si-O-Si from the PGS nanoparticles, making the modified surface chemically inert. The lowest surface free energy was found in M-5, attributed to the highest Si elemental composition of 44.7% on the membrane surface. This implies the weakest affinity towards water molecules, hence provides the highest surface hydrophobicity [14].

Surface wetting resistance of the fabricated membrane was characterized via the contact angle measurement, as reported in Fig. 4. Unmodified membrane, M-0, exhibited the lowest water contact angle of 134±1.08° due to high surface free energy and low surface roughness [15]. Upon addition of PGS additives, all modified membranes exhibited impressive hydrophobicity, where the contact angle values were remarkably enhanced to the range of 142±1.12°-161±1.98°. The membrane successfully achieved superhydrophobic surface exceeding contact angle of 150° at PGS concentration higher than 3 gL^{-1}. Such disparity in water contact angle and wetting resistance is ascribed to the multilevel surface protrusion and decrease in surface free energy. Membrane with low surface free energy contributes to a substantial reduction in interaction with liquid molecules, hence decreases the adhesion of the liquid droplet on the membrane surface [16]. Meanwhile, texture surface encloses the air pockets between patchwork of solid clusters, so liquid molecules with capillary force tend to bridge across the multilevel protrusion [17]. Both factors reduce the footprint of water molecules on the membrane surface, amplifying the hydrophobicity towards superhydrophobiciy. The maximum contact angle of 161±1.98° was attained in M-5, showing significant improvement of 16.4% compared to unmodified membrane. It is observed that further increase in non-solvent additive concentration, however, did not enhance the water contact angle due to significant agglomeration.

The stability of the deposition layer plays an important role in maintaining the hydrophobicity of the modified membranes. In membrane gas-liquid separation process (i.e., desalination, distillation and gas absorption), membranes are exposed to different temperatures and fluid velocity, which could detach the loosely deposited nanoparticles. Therefore, thermal and mechanical tests were performed to investigate the stability of deposition layer. Fig. 5 demonstrates the thermal stability of membranes. It is observed that the contact angle of modified membranes decreased gradually with increasing cycle times, whereby no sharp reduction was observed.

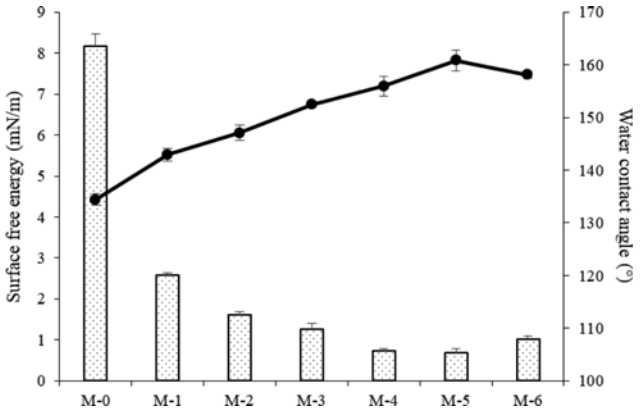

Fig. 4. Water contact angle and surface free energy of membrane.

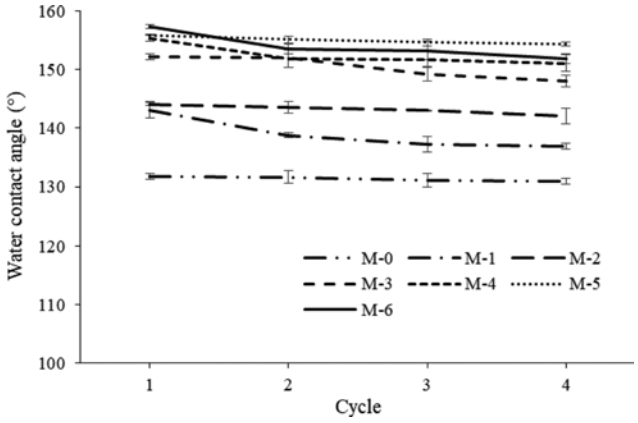

Fig. 5. Water contact angle of membranes after exposure to four cycles of thermal test.

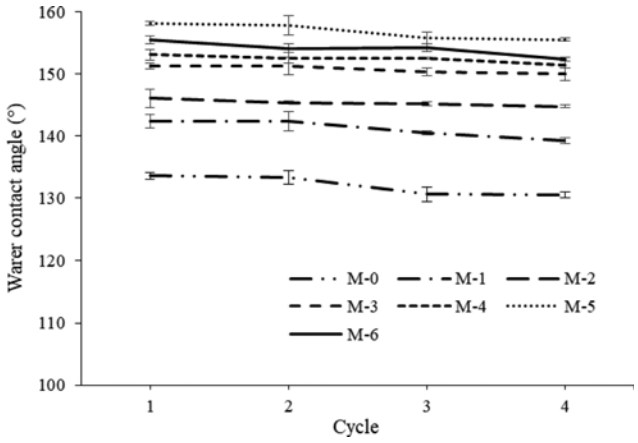

Fig. 6. Water contact angle of membranes after exposure to four cycles of mechanical test.

After four cycles, all the modified membranes exhibited a decrease by less than 5% in contact angle. When the PGS concentration was greater than 4 g, the modified membrane retained superhydrophobic property. Therefore, it can be deduced that the deposition layer exhibited good thermal stability and durability, which is important for practical application. Similarly, a slight decrease of contact angle was observed in modified membranes at the end of the mechanical tests (Fig. 6). This was probably due to leaching of some loosely attached large residues from the surface. Nevertheless, the contact angle of modified membranes was reduced by less than 4%, indicating the deposition of nanoparticles was mechanically stable.

CONCLUSION

Superhydrophobic membrane was successfully developed by generating hierarchical structure and reducing the membrane surface free energy via PGS incorporation. However, when the PGS loading exceeded 5 gL^{-1}, significant aggregation of silica nanoparticles was observed, which led to the reduction in contact angle. Therefore, the optimal concentration was determined at 5 gL^{-1} for this study. The modified membranes also exhibited superior mechanical and thermal resistance. These results confirmed that PGS modified membranes have the potential to be used in membrane gas-liquid separation processes for enhanced anti-wettability.

ACKNOWLEDGEMENT

This research work was supported by Universiti Teknologi PETRONAS under YUTP-FRG grant no. 0153AA-E08 and FRGS grant no 015MA0-003.

REFERENCES

1. S. Mosadegh-Sedghi, D. Rodrigue, J. Brisson and M. C. Iliuta, *J. Membr. Sci.*, **452**, 332 (2014).
2. J. K. J. Yong, The Development of Thin Films for Efficient Carbon Capture and Storage, M.S. thesis, University of Melbourne Victoria (2016).
3. H. Nurul Faiqotul and I. G. Wenten, *J. Phys: Conf. Ser.*, **877**, 10 (2017).
4. M. H. Ibrahim, M. H. El-Naas, Z. Zhang and B. Van der Bruggen, *Energy Fuels*, **32**, 963 (2018).
5. J. Jeevahan, M. Chandrasekaran, G. B. Joseph, R. Durairaj and G. Mageshwaran, *J. Coat. Technol. Res.*, **15**, 231 (2018).
6. X. Wu, B. Zhao, L. Wang, Z. Zhang, J. Li and X. He, *Sep. Purif. Technol.*, **190**, 108 (2018).
7. A. Ghaee, A. Ghadimi, B. Sadatnia, A. F. Ismail, Z. Mansourpour and M. Khosravi, *Chem. Eng. Res. Des.*, **120**, 47 (2017).
8. G. Y. E. Tan, P. C. Oh, K. K. Lau and S. C. Low, *Chin. J. Polym. Sci.*, **37**, 654 (2019).
9. V. Fernández and M. Khayet, *Frontiers in Plant Sci.*, **6**, 510 (2015).
10. I. Malavasi, I. Bernagozzi, C. Antonini and M. Marengo, *Surf. Innovations*, **3**, 49 (2014).
11. Y. Liu, T. Xiao, C. Bao, Y. Fu and X. Yang, *J. Membr. Sci.*, **563**, 298 (2018).
12. S. Munirasu, F. Banat, A. A. Durrani and M. A. Haija, *Desalination*, **417**, 77 (2017).
13. B. Dong, L. Yang, Q. Yuan, Y. Liu, J. Zhang and G. Fang, *Construction and Building. Mater.*, **110**, 163 (2016).
14. C. Boo, J. Lee and M. Elimelech, *Environ. Sci. Technol.*, **50**, 8112 (2016).
15. G. B. Darband, M. Aliofkhazraei, S. Khorsand, S. Sokhanvar and A. Kaboli, *Arabian. J. Chem.* (2018), doi:10.1016/j.arabjc.2018.01.013.
16. K. Y. Eum, I. Phiri, J. W. Kim, W. San Choi, J. M. Ko and H. Jung, *Korean J. Chem. Eng.*, **36**, 1313 (2019).
17. H. Zhou, R. Shi and W. Jin, *Sep. Purif. Technol.*, **127**, 61 (2014).